Binary Conformational Switches in a Porphyrin Chain: Tautomerization and Stereoisomerization

Zhijing Feng,[†,¶,1] *Simone Velari,*[‡,2] *Carlo Dri,*[†,¶,3] *Andrea Goldoni,*[Δ] *Maria Peressi,*[†,*] *and Giovanni Comelli*[†,¶]

[†] Department of Physics, University of Trieste, Via A. Valerio 2, I-34127 Trieste, Italy

[¶] TASC Laboratory, Istituto Officina dei Materiali IOM-CNR, S.S. 14 – km 163.5, I-34149 Trieste, Italy

[‡] Department of Engineering and Architecture, University of Trieste, Via A. Valerio 6/1, I-34127 Trieste, Italy

[Δ] Elettra-Sincrotrone Trieste, Area Science Park, S.S.14 – km 163.5, I-34149 Trieste, Italy

ABSTRACT: In the last decade, hydrogen (H-)tautomerization *i.e.* a reaction that involves simple intramolecular proton transfer, has been studied in single phthalocyanine, porphyrin, and porphycene derivatives as a prototypical single molecular conductance switch. Here, by means of low temperature scanning tunneling microscopy and density functional theory calculations, we report a binary H-tautomerism and stereoisomeric conformational switch in (amino-functionalized) porphyrins assembled in molecular chains on a gold surface. We show that the formation of the chain is crucial for the binary tautomeric switch mechanism as the single molecule switches differently. Our findings suggest that the (amino-)functionalization of molecules can be exploited not only to drive the formation of molecular self-assemblies but also to steer their switching properties.

Introduction

The miniaturization of electronic devices into single molecules is one of the ultimate goals of molecular electronics and physical chemistry. To be useful for potential devices, a molecule must exhibit specific electronic properties such as, for instance, switching or rectification.[1] Moreover, the same molecule must be positioned and interconnected to other molecules within an electric circuit. To this aim, researchers worldwide devote considerable efforts in studying on the one side the interaction between molecules via covalent,[2,3] metal-organic[4–7] or hydrogen bonds[8,9] and, on the other side, their switching[10–14] or rectification[15] properties on surfaces. In this context, single phthalocyanine, porphyrin, and porphycene derivatives have been proposed as single molecule switches, where inner hydrogen tautomerization[10,16–18] or molecule conformational change[19–23] on a metal substrate are at the basis of the conductance change.[24,25]

In a recent work[26] we showed that aminophenyl-functionalized porphyrins (called TAPPs, **Figure 1a**) deposited on a gold (111) surface form weakly bonded chains via hydrogen bonds between their amino-terminations. We described the chemical and electronic structure of the TAPP chains, which was strongly influenced by the interplay between the amino-amino and amino-gold substrate interactions.

In the present work, by means of low temperature scanning tunneling microscopy (LT-STM) and *ab initio* calculations based on Density Functional Theory (DFT), we investigate the switching properties of each TAPP molecule along these chains. Our work shows that scanning probe microscopy is a powerful tool not only for characterizing but also for manipulating the transport properties of TAPPs at the atomic level, following the lines of previous results reported on similar molecules.[27] Additionally, we find that the formation of the chain is crucial for the switching properties of the molecules, which depend also on the protonation state of the inner macrocycle: only partially deprotonated donor-TAPPs can undergo H-tautomerization, while fully deprotonated TAPPs can undergo a binary stereoisomeric conformational switch.

Methods

Experimental methods

As in our previous work[26], experiments were performed in ultra high vacuum (UHV) conditions at a base pressure of 1×10^{-8} Pa. 5,10,15,20-tetra(4-aminophenyl)porphyrin (abbreviated TAPP, PorphyChem, purity 98%, see Figure 1a) were evaporated from a Knudsen cell at 520 – 570 K on a clean monocrystalline Au(111) sample at room temperature. The Au(111) sample was previously cleaned via standard Ne^+ ion sputtering and annealing to 870 K for 10 minutes. STM imaging was performed with an Omicron Low Temperature STM,

operating at a temperature of approximately 4.3 K. Images were acquired in the constant current mode, and the bias reported in the images is given with respect to the sample, *i.e.* a positive bias indicates imaging of the empty states of the sample. Electrochemically etched tungsten tips were used for imaging.

Computational approach

DFT calculations were performed with the plane-wave pseudopotential package QUANTUM ESPRESSO[28] using GGA-PBE[29] ultrasoft pseudopotentials.[30] The wave function energy cut-off was set at 30 Ry. Considering the large size of the cell, the Brillouin-zone sampling included only the gamma point. Since van der Waals interactions play a non-negligible role in self-assembled organic structures, the calculations were performed including the semi-empirical dispersion-corrected DFT (DFT-D) method proposed by Grimme,[31] implemented in the QE package[32] and already used by us in our previous work.[26]

The Au(111) surface was modeled with a two-layer slab at the bulk Au calculated structure (lattice parameter a_{bulk}=0.407 nm, equal to the experimental one) to mimic the behavior of the metal substrate. Slabs were separated by a vacuum spacing of ≈ 1.4 nm. The two gold layers were kept fixed, except for the gold atoms underneath the center of the porphyrins. We simulated the TAPP chain using the smallest periodically repeated unit cell commensurated with the substrate and compatible with the experimental chain period, containing two adjacent TAPP molecules: one acceptor and one donor, according to the definition given in our previous work.[26] The acceptor was always the same, and we focused on different configurations and conformations of the donor. All the atoms of the porphyrins were allowed to relax until the calculated forces acting on each one were smaller than 0.26 eV/Å. STM images were simulated

within the Tersoff-Hamann[33] approximation, using the energy-integrated local density of states (ILDOS) and mapping its iso-surfaces to simulate the experimental "constant current" condition. The images were simulated at various biases, at an ILDOS value for the iso-surface of 10^{-6} nm^{-3}, lying at an average distance of approximately 0.5 nm from the outmost atomic layer.

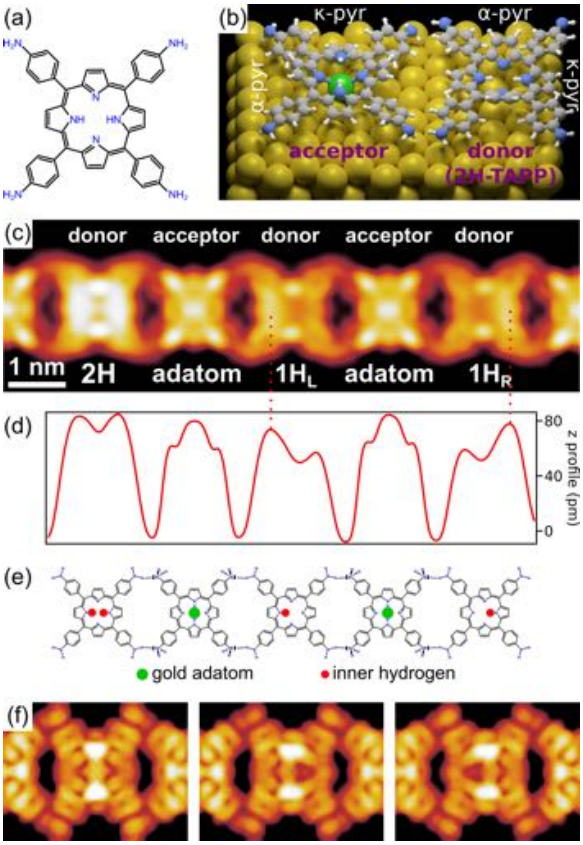

Figure 1. (a) Chemical structure of 5,10,15,20-tetra(4-aminophenyl)porphyrin (TAPP). (b) Stick and ball model of a TAPP chain obtained by the DFT calculations. The gold adatom trapped by the acceptor is highlighted in green. The κ-pyrroles and α-pyrroles are labelled κ-pyr and α-pyr, respectively, with the inner hydrogens located on the two κ-pyrroles. (c-d) High resolution STM image (c) of a section of a TAPP chain together with its z-profile (d), measured along the horizontal symmetry axis of the chain, that highlights the asymmetry of the 1H-TAPPs. Chemical structure model (e) of the same TAPP chain, where the donor-acceptor model and the

different internal structures of each TAPP are showed. From left to right: donor with both inner hydrogen (2H), acceptor with one gold adatom, donor with one inner hydrogen (1H), acceptor with one gold adatom, donor with one inner hydrogen (1H). (f) simulated STM images of the DFT-optimized configurations of units of a TAPP chain with 2H, $1H_L$, and $1H_R$ donor, whose combination are equivalent to (e). Image parameters: (d) $V = -0.2$ V, $I = 0.5$ nA, 10×3 nm^2.

Results and Discussion

When deposited on Au(111), the TAPP molecules spontaneously form chains along the herringbone reconstruction of the substrate. The structure of these chains has already been described in our previous work.[26] In a nutshell, TAPPs form such chains via amino-amino hydrogen bonds between their aminophenyl-terminations. In these chains, TAPPs behave alternately as a hydrogen donor and acceptor as a whole. Moreover, in the STM images, most acceptors have a bright protrusion at their center, which, by comparing experimental and simulated STM images, was associated to a gold adatom trapped underneath via a coordination bond between the N atoms of two pyrroles and the adatom. **Figure 1b** shows a stick and ball model of the system: opposite pairs of pyrroles are labelled α-pyrrole (tilted downwards) or κ-pyrrole (tilted upwards) according to their angle with respect to the substrate.[34]

The high resolution STM image in **Figure 1c** shows a detail of five TAPP molecules in a chain, with a z-profile (**Figure 1d**), acquired along the horizontal symmetry axis of the chain, highlighting the different symmetries of each TAPP. Whereas the two acceptors have an identical symmetric z-profile, for the donors the situation changes. More specifically, the donor on the left is symmetric, being characterized by two equal peaks, whereas the other two donors have two specular asymmetric profiles. By comparing our STM images with previous results

from literature,[10] we hypothesize that the asymmetric TAPPs correspond to partially deprotonated molecules, which have lost one inner hydrogen (see also **Figure 1e**), thus named 1H-TAPP. In the works reported in literature,[10,17,18,35–37] when there is an asymmetry in the STM images due to the presence of hydrogen atoms, the brighter side is associated to their position. Therefore, following the model in **Figure 1e** from left to right, we suppose that the first donor TAPP has both inner protons (2H), the second donor has a single inner proton on the left κ-pyrrole ($1H_L$), and the last donor has a single inner proton on the right κ-pyrrole ($1H_R$). The simulated STM image (**Figure 1f**) of the DFT-optimized model is in satisfactory agreement with the observations, thus confirming our picture of partially deprotonated donors. We point out that, compared to our previous work about such TAPP chains,[26] in the present work we performed STM imaging at a lower bias voltage of −0.2 V, which provides a slightly better contrast between the $1H_L$- and the $1H_R$-TAPPs, and the simulations are performed accordingly.

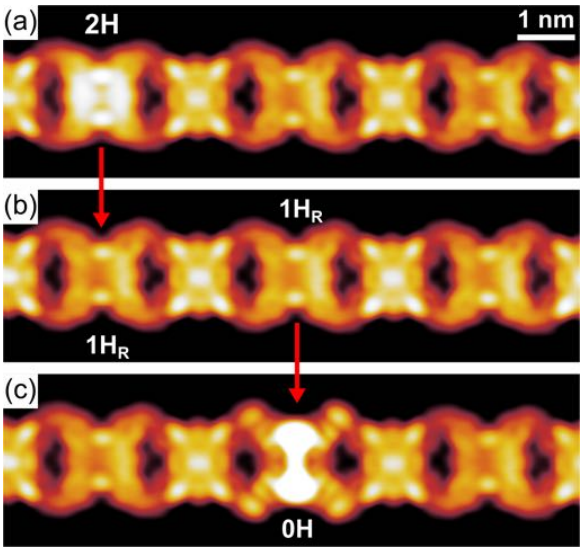

Figure 2. Sequential deprotonation of single TAPP molecules in a TAPP chain on Au(111). (a) A 2H-TAPP is deprotonated into (b) a 1H-TAPP by applying a −1.2 V bias pulse on the center of

the molecule. (b) A 1H-TAPP is deprotonated into an (c) 0H-TAPP by applying a −2.0 V bias pulse on the center of the molecule. Image parameters: $V = -0.2$ V, $I = 0.5$ nA, 10×3 nm^2.

To obtain the deprotonated TAPPs described above, we performed single molecule voltage-pulse manipulation with the STM tip. **Figure 2** shows a sequence of three STM images where controlled deprotonation of selected TAPP donors was obtained by centering the STM tip above the molecule and increasing the bias voltage over a specific threshold, as previously reported.[10] Following this procedure, a 2H-TAPP (**Figure 2a**) is deprotonated into an 1H-TAPP (Figure 2b) by applying a –1.2 V bias pulse onto the center of the molecule. Subsequently, an 1H-TAPP (**Figure 2b**) is deprotonated into a 0H-TAPP (**Figure 2c**) by applying a –2.0 V bias pulse onto the center of the molecule. The latter reactions were irreversible, as we never observed a 0H-TAPP reverting back to 1H-TAPP nor a 1H-TAPP reverting back to 2H-TAPP, in agreement with the assumption that these reactions are dehydrogenations. We must point out that the first stage of deprotonation, *i.e.* from 2H-TAPP to 1H-TAPP, is also induced thermally when TAPP is sublimed at 520 – 570 K from the UHV evaporator. Indeed, in our images we find most of the donors as 1H-TAPP, *i.e.* already partially deprotonated, while 2H-TAPPs are less commonly observed. However, 0H-TAPPs are never spontaneously formed on Au(111), suggesting that the thermal energy available during deposition is insufficient to overcome the barrier involved in the removal of the second proton.

DFT calculations suggest that the dehydrogenation energy barriers are rather high: we did not calculate them precisely, but from total energy differences (initial configuration compared with a corresponding configuration with one hydrogen removed from the molecule but still present in

the simulation cell) we estimate barriers of about 5.0 and 5.2 eV for the first and the second dehydrogenation, respectively. These values cannot be directly compared with the experimental deprotonation thresholds, but at least are consistent with the higher energy required for the second deprotonation.

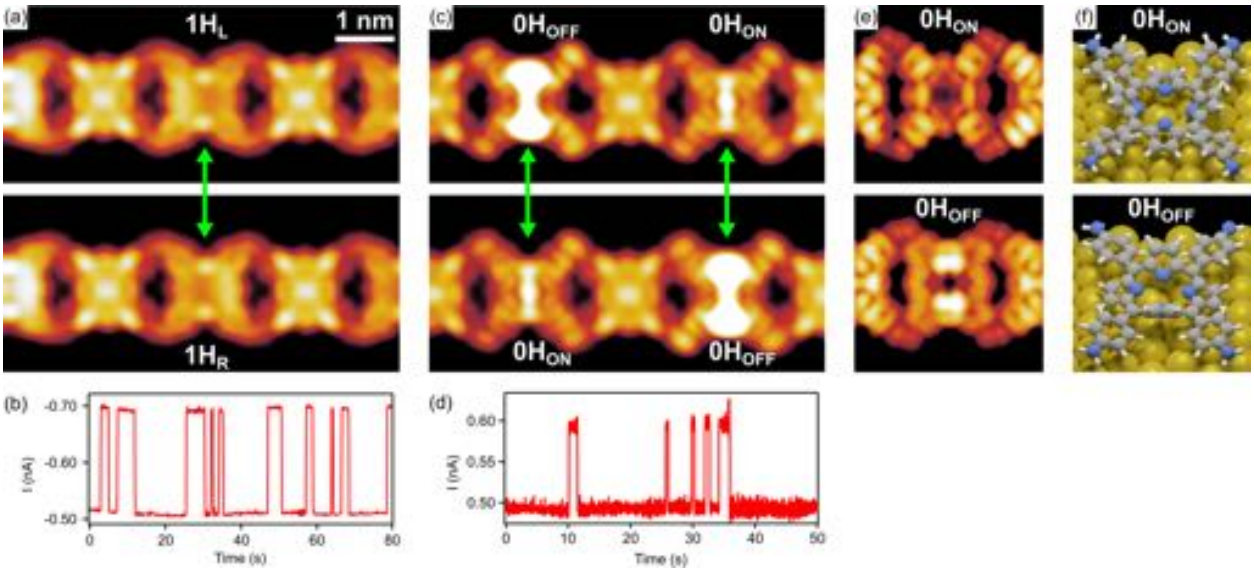

Figure 3. Switching in 1H-TAPP and 0H-TAPP. (a) Binary H-tautomerization in the central 1H-TAPP and (b) *I(t)* trace recorded on it at bias of −1.5 V (the current values are negative because of the negative bias). (c) Binary stereoisomeric conformational switch in two 0H-TAPPs and (d) a typical *I(t)* trace recorded at their center at bias +1.0 V. (e) Simulated STM image of the DFT-optimized model in (f). (f) DFT-optimized model illustrating the stereoisomeric conformation switch of a 0H-TAPP, where all the pyrroles change their orientation: for the pyrroles labeled α (Figure 1b) in the OFF state, the tilting angle changes from −47° (N pointing downwards) to +22° (N upwards) in the ON state; for those labeled κ in the OFF state, it changes from +24° (N upwards) to −42° (N downwards). For the sake of clarity, only the atoms of the 0H-TAPP are

shown, extracted from a chain model. Image parameters: (a) and (c) $V = -0.2$ V, $I = 0.5$ nA, 10×3 nm^2.

In a subsequent stage, we studied the H-tautomerization of the inner protons in each TAPP within such chains. The reaction can be induced by positioning the STM tip above the molecule and increasing the bias voltage below the HOMO or above the LUMO resonance of the molecule,[16] while simultaneously monitoring the current signal in the constant height mode, *i.e.* recording the current versus time *I(t)* spectra. In this way, the tautomerization reaction is induced by vibrational excitation via inelastic electron tunneling into the molecules,[16,38] with different current values associated to different proton positions. In the acceptor TAPPs no H-tautomerization switching was found, likely due to the presence of the central Au adatoms which hinder this process. In the donors we never observed switching within 2H-TAPPs, while we found a binary H-tautomerism in 1H-TAPPs where the inner hydrogen atom can "jump" only between the κ-pyrroles, as shown in **Figure 3a-b**.

These findings are in contrast to what described so far in the literature for individual molecules, where the 2H-tetraphenylporphyrin,[9] 2H-phthalocyanine,[15,36] and 2H-porphycenes[17,18,39] are reported to be switchable and 1H-tetraphenylporphyrin can switch into all 4 pyrroles sites.[10] Apparently, here, in the donors, the hydrogen atoms can bind only to κ-pyrroles and switch between them. Although our DFT simulations did not exclude the possibility of hydrogen atoms bonded to the α-pyrroles, the optimized chain model showed a better resemblance with the experimental observations when hydrogen atoms are bonded to κ-pyrroles.[26] In conclusion, since the H-switching channels in each molecule seem to be inhibited

by the geometry of the TAPPs within the chains, which is mainly dictated by the aminophenyl terminations, we deduce that the aminophenyl functionalization indirectly influences also the symmetry of the H-switching properties within the molecules.

Interestingly, we found that also the fully deprotonated 0H-TAPP is switchable in two different states, which we call $0H_{OFF}$ and $0H_{ON}$, as shown in **Figure 3c-f**. This switching behavior cannot be due to tautomerization, as there are no inner protons left. Therefore, it must reflect a molecule's stereoisomeric conformational change. It is known that porphyrins can undergo a conformational switching under electric field or inelastic electron tunneling.[19,20,23] Here, the strong contrast change at the α-pyrroles positions after a switching event, shown in **Figure 3c**, suggests an important change of their tilting angle. The DFT simulations indeed indicate for the 0H-TAPPs in the chain the possibility of two conformations with reversed molecular saddle shape (**Figure 3f**), notwithstanding the geometrical constraint imposed by the amino-amino and amino-gold interaction. For the structural point of view, the $0H_{OFF}$ conformation is very similar to the 2H-TAPP, with the pyrroles tilting angles slightly larger in the former: this indicates that the strong difference in the STM images, also reproduced by the DFT simulations (**Figure 3e**), is mainly due to electronic rather than geometrical effects. The relevance of the electronic effect is confirmed also by the electron density distribution analyzed in detail in **Figures S1** and **S2**, which significantly changes under switching. The $0H_{ON}$ conformation is characterized by a switch of the pyrroles orientation in the inner macrocycle: for the pyrroles labeled α in the $0H_{OFF}$ state, the tilting angle changes from −47° (N pointing downwards) to +22° (N upwards) in the $0H_{ON}$ state; for those labeled κ in the $0H_{OFF}$ state, it changes from +24° (N upwards) to −42° (N downwards). Furthermore, also the amino-phenyl terminal groups switch their tilting angle. The net result is almost equivalent to a 90° rotation of the molecule along its symmetry axis

perpendicular to the surface. The $0H_{ON}$ conformation is stable, but about 1 eV higher in energy than $0H_{OFF}$, consistent with its observation only after a voltage pulse has been applied, although a direct comparison with the experimental threshold for switching cannot be established. As in the experimental STM image, also in the DFT simulated image of the $0H_{ON}$ conformation the bright feature associated to the α-pyrroles has almost disappeared.

Figure 3b shows a typical *I(t)* (current versus time) trace recorded on a 1H-TAPP with –1.5 V bias, where the two current values correspond to the binary switching between $1H_L$ and $1H_R$. The switching rate and ratio between the two states depend on the bias value and tip position applied to 1H-TAPP. In a *I(t)* trace, the state characterized by the highest current value (absolute value) is characterized also by the shortest duration (in Figure 3b the state associated to the –0.70 nA current lasts less than the one with –0.50 nA) since higher current value means more tunneling electrons, and thus higher probability of inelastic tunneling. The *I(t)* traces always display two different values because the tip is centered asymmetrically, either closer to the left or to the right κ-pyrrole. **Figure 3d** shows a typical *I(t)* trace recorded on the center of a 0H-TAPP at +1 V bias, where the two current values correspond to the binary switching between $0H_{OFF}$ and $0H_{ON}$. Here, the *I(t)* trace suggests that one state is less stable than the other, since there is no asymmetry of the inner protons argument to justify the observed behavior. By comparing the STM images before and after *I(t)* traces we conclude that the most stable state is $0H_{OFF}$, as predicted by DFT.

We point out that single TAPPs were challenging to manipulate as they were mobile on surface, while in the monolayer phase, 2H-TAPP can undergo reversible stereoisomeric conformational change (**Figure S3**), while 2H-TAPP trapping adatoms can cause irreversible metalation (Figure S3), similarly to recent literature reporting 2H-tetraphenylporphyrins.[23,40] The

latter findings further support the hypothesis of the influence of the aminophenyl functionalization on the H-switching properties within the molecules.

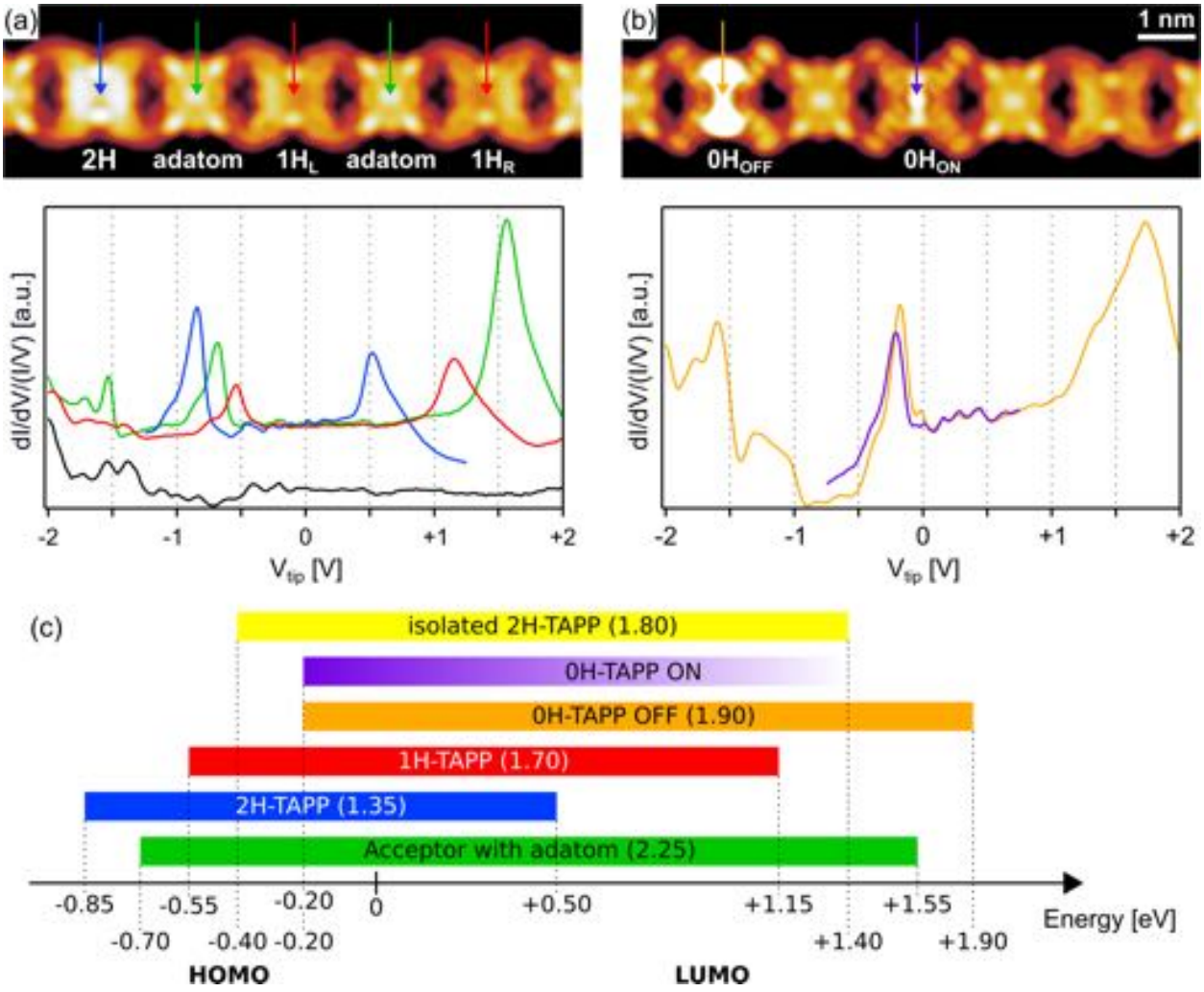

Figure 4. STS spectra recorded at the center of single molecules in TAPP chains, where each color indicates a different type of TAPP. (a) STS spectra of 2H-TAPP (blue), acceptor TAPP trapping an adatom (green), and 1H-TAPP (red). The blue spectrum is limited in the [−1.25; +1.25] V range, otherwise 2H-TAPP undergoes deprotonation. The black spectrum at the bottom is acquired the Au(111) substrate for comparison. (b) STS spectra of $0H_{OFF}$ (orange) and $0H_{ON}$ (violet). The violet spectrum is limited in the [−0.75; +0.75] V range because for higher bias

$0H_{ON}$ switches to $0H_{OFF}$. (c) Graph showing the HOMO and LUMO energies of various types of TAPP and the relative HOMO-LUMO gaps in eV in the brackets.

Finally, we performed scanning tunneling spectroscopy (STS) experiments to study the electronic structure changes of the different 2H-, 1H-, 0H- TAPPs. **Figure 4a, b** show STS spectra recorded at the center of single molecules in TAPP chains, where every TAPP in the chain has a different electronic structure with respect to single isolated TAPP molecules (**Figure 4c**). 1H-TAPP has both the HOMO and LUMO shifted towards higher energies (**Figure 4a**) with respect to 2H-TAPP and a wider HOMO-LUMO gap, suggesting that deprotonation affects the transport properties of molecules on surface by shifting both HOMO and LUMO to higher energies. Because of the symmetry of the system, both $1H_L$ and $1H_R$ tautomers display the same STS spectrum. Similarly, 0H-TAPP ($0H_{OFF}$) has both HOMO and LUMO shifted towards higher energies and a wider HOMO-LUMO gap with respect to 1H-TAPP (**Figure 4b**). As discussed in our previous work,[26] the acceptor TAPP trapping an adatom at its center has the largest HOMO-LUMO gap, which is in agreement with the reduced extent of conjugation occurring in the acceptors.

Conclusions

Summarizing, in the present work by means of LT-STM and DFT simulations we have investigated the switching properties of TAPP molecular chains, exploiting both H-tautomerism and conformation change. The partially deprotonated 1H-TAPP is found to be characterized by a binary H-tautomerization switch on the κ-pyrroles along the TAPP chain. Moreover, the fully

deprotonated 0H-TAPP is shown to be switchable into two different conformational geometries. The interplay between the amino-amino and amino-gold substrate interaction dictates the geometry of each molecule and thereby the number of switching channels available for the H-tautomerization reaction and conformational change. The STS shows that deprotonation affects the transport properties of molecules on surface by shifting both HOMO and LUMO to higher energies and increasing the HOM-LUMO gap. Our studies reveal the role of the molecular functionalization in determining the self-assembly and consequently the switching properties in molecules, thus suggesting a novel criterion to control single molecule switches by exploiting the molecule-molecule and molecule-substrate interactions.

ASSOCIATED CONTENT

Supporting Information Description

Supporting Information is available is available free of charge on the ACS Publications website at DOI: 10.1021/**********

DFT calculated electron density rearrangement due to the chain-substrate interaction in the TAPP chain on Au(111) for different protonation and switching states of the donor molecule: isosurfaces and average profiles. STM images of a compact monolayer of TAPP where different molecules are modified by applying voltage pulses.

AUTHOR INFORMATION

Corresponding Author

* E-mail: (M.P.) peressi@ts.infn.it

ORCID

Zhijing Feng: 0000-0002-8778-8878

Carlo Dri: 0000-0001-9040-5746

Andrea Goldoni: 0000-0001-9989-3889

Maria Peressi: 0000-0001-6142-776X

Giovanni Comelli: 0000-0003-4603-2094

Present Addresses

[1] Z.F.: Department of Chemical Engineering and Materials Science, University of California, Irvine, Irvine, CA 92697, USA

[2] S.V.: Modefinance, AREA Science Park, Località Padriciano 99, I-34149 Trieste, Italy

[3] C.D.: ELETTRA-Sincrotrone Trieste, S.S. 14 km 163.5, Basovizza, I-34149 Trieste, Italy

Author Contributions

The manuscript was written through contributions of all authors. All authors have given approval to the final version of the manuscript.

Notes

The authors declare no competing financial interest.

ACKNOWLEDGMENTS

M.P. acknowledges the University of Trieste through the program "Finanziamento di Ateneo per progetti di ricerca scientifica – FRA 2018". Computational resources have been obtained from the CINECA Consortium through the ISCRA initiative and the agreement with the University of Trieste.

References

(1) Stuyver, T.; Perrin, M.; Geerlings, P.; De Proft, F.; Alonso, M. Conductance Switching in Expanded Porphyrins through Aromaticity and Topology Changes. *J. Am. Chem. Soc.* **2018**, *140*, 1313–1326.

(2) Grill, L.; Dyer, M.; Lafferentz, L.; Persson, M.; Peters, M. V; Hecht, S. Nano-Architectures by Covalent Assembly of Molecular Building Blocks. *Nat. Nanotechnol.* **2007**, *2*, 687–691.

(3) Lafferentz, L.; Eberhardt, V.; Dri, C.; Africh, C.; Comelli, G.; Esch, F.; Hecht, S.; Grill, L. Controlling On-Surface Polymerization by Hierarchical and Substrate-Directed Growth. *Nat. Chem.* **2012**, *4*, 215–220.

(4) Klappenberger, F.; Weber-Bargioni, A.; Auwärter, W.; Marschall, M.; Schiffrin, A.; Barth, J. V. Temperature Dependence of Conformation, Chemical State, and Metal-Directed Assembly of Tetrapyridyl-Porphyrin on Cu(111). *J. Chem. Phys.* **2008**, *129*, 214702.

(5) Shi, Z.; Lin, N. Porphyrin-Based Two-Dimensional Coordination Kagome Lattice Self-Assembled on a Au(111) Surface. *J. Am. Chem. Soc.* **2009**, *131*, 5376–5377.

(6) Fendt, L.-A.; Stöhr, M.; Wintjes, N.; Enache, M.; Jung, T. A.; Diederich, F. Modification of Supramolecular Binding Motifs Induced By Substrate Registry: Formation of Self-

Assembled Macrocycles and Chain-Like Patterns. *Chem. - A Eur. J.* **2009**, *15*, 11139–11150.

(7) Heim, D.; Seufert, K.; Auwärter, W.; Aurisicchio, C.; Fabbro, C.; Bonifazi, D.; Barth, J. V. Surface-Assisted Assembly of Discrete Porphyrin-Based Cyclic Supramolecules. *Nano Lett.* **2010**, *10*, 122–128.

(8) Feng, Z.; Castellarin Cudia, C.; Floreano, L.; Morgante, A.; Comelli, G.; Dri, C.; Cossaro, A. A Competitive Amino-Carboxylic Hydrogen Bond on a Gold Surface. *Chem. Commun.* **2015**, *51*, 5739–5742.

(9) Yokoyama, T.; Yokoyama, S.; Kamikado, T.; Okuno, Y.; Mashiko, S. Selective Assembly on a Surface of Supramolecular Aggregates with Controlled Size and Shape. *Nature* **2001**, *413*, 619–621.

(10) Auwärter, W.; Seufert, K.; Bischoff, F.; Ecija, D.; Vijayaraghavan, S.; Joshi, S.; Klappenberger, F.; Samudrala, N.; Barth, J. V. A Surface-Anchored Molecular Four-Level Conductance Switch Based on Single Proton Transfer. *Nat. Nanotechnol.* **2012**, *7*, 41–46.

(11) Choi, B.-Y.; Kahng, S.-J.; Kim, S.; Kim, H.; Kim, H. W.; Song, Y. J.; Ihm, J.; Kuk, Y. Conformational Molecular Switch of the Azobenzene Molecule: A Scanning Tunneling Microscopy Study. *Phys. Rev. Lett.* **2006**, *96*, 156106.

(12) Dri, C.; Peters, M. V.; Schwarz, J.; Hecht, S.; Grill, L. Spatial Periodicity in Molecular Switching. *Nat. Nanotechnol.* **2008**, *3*, 649–653.

(13) Godlewski, S.; Kawai, H.; Kolmer, M.; Zuzak, R.; Echavarren, A. M.; Joachim, C.; Szymonski, M.; Saeys, M. Single-Molecule Rotational Switch on a Dangling Bond Dimer Bearing. *ACS Nano* **2016**, *10*, 8499–8507.

(14) Simpson, G. J.; Hogan, S. W. L.; Caffio, M.; Adams, C. J.; Früchtl, H.; van Mourik, T.; Schaub, R. New Class of Metal Bound Molecular Switches Involving H-Tautomerism. *Nano Lett.* **2014**, *14*, 634–639.

(15) Capozzi, B.; Xia, J.; Adak, O.; Dell, E. J.; Liu, Z.-F.; Taylor, J. C.; Neaton, J. B.; Campos, L. M.; Venkataraman, L. Single-Molecule Diodes with High Rectification Ratios through Environmental Control. *Nat. Nanotechnol.* **2015**, *10*, 522–527.

(16) Liljeroth, P.; Repp, J.; Meyer, G. Current-Induced Hydrogen Tautomerization and Conductance Switching of Naphthalocyanine Molecules. *Science* **2007**, *317*, 1203–1206.

(17) Waluk, J. Spectroscopy and Tautomerization Studies of Porphycenes. *Chem. Rev.* **2017**, *117*, 2447–2480.

(18) Fita, P.; Grill, L.; Listkowski, A.; Piwoński, H.; Gawinkowski, S.; Pszona, M.; Sepioł, J.; Mengesha, E.; Kumagai, T.; Waluk, J. Spectroscopic and Microscopic Investigations of Tautomerization in Porphycenes: Condensed Phases, Supersonic Jets, and Single Molecule Studies. *Phys. Chem. Chem. Phys.* **2017**, *19*, 4921–4937.

(19) Moresco, F.; Meyer, G.; Rieder, K.-H.; Tang, H.; Gourdon, A.; Joachim, C.

Conformational Changes of Single Molecules Induced by Scanning Tunneling Microscopy Manipulation: A Route to Molecular Switching. *Phys. Rev. Lett.* **2001**, *86*, 672–675.

(20) Qiu, X. H.; Nazin, G. V.; Ho, W. Mechanisms of Reversible Conformational Transitions in a Single Molecule. *Phys. Rev. Lett.* **2004**, *93*, 196806.

(21) Wang, Y.; Kröger, J.; Berndt, R.; Hofer, W. A. Pushing and Pulling a Sn Ion through an Adsorbed Phthalocyanine Molecule. *J. Am. Chem. Soc.* **2009**, *131*, 3639–3643.

(22) Stadler, C.; Hansen, S.; Kröger, I.; Kumpf, C.; Umbach, E. Tuning Intermolecular Interaction in Long-Range-Ordered Submonolayer Organic Films. *Nat. Phys.* **2009**, *5*, 153–158.

(23) Pham, V. D.; Repain, V.; Chacon, C.; Bellec, A.; Girard, Y.; Rousset, S.; Abad, E.; Dappe, Y. J.; Smogunov, A.; Lagoute, J. Tuning the Electronic and Dynamical Properties of a Molecule by Atom Trapping Chemistry. *ACS Nano* **2017**, *11*, 10742–10749.

(24) Jan van der Molen, S.; Liljeroth, P. Charge Transport through Molecular Switches. *J. Phys. Condens. Matter* **2010**, *22*, 133001.

(25) Jurow, M.; Schuckman, A. E.; Batteas, J. D.; Drain, C. M. Porphyrins as Molecular Electronic Components of Functional Devices. *Coord. Chem. Rev.* **2010**, *254*, 2297–2310.

(26) Feng, Z.; Velari, S.; Dri, C.; Goldoni, A.; Patera, L. L.; Regeni, I.; Forzato, C.; Berti, F.; Peressi, M.; De Vita, A.; et al. Bifunctional Behavior of a Porphyrin in Hydrogen-Bonded Donor–Acceptor Molecular Chains on a Gold Surface. *J. Phys. Chem. C* **2019**, *123*, 7088–7096.

(27) Niu, T.; Li, A. Exploring Single Molecules by Scanning Probe Microscopy: Porphyrin and Phthalocyanine. *J. Phys. Chem. Lett.* **2013**, *4*, 4095–4102.

(28) Giannozzi, P.; Baroni, S.; Bonini, N.; Calandra, M.; Car, R.; Cavazzoni, C.; Ceresoli, D.; Chiarotti, G. L.; Cococcioni, M.; Dabo, I.; et al. QUANTUM ESPRESSO: A Modular and Open-Source Software Project for Quantum Simulations of Materials. *J. Phys. Condens. Matter* **2009**, *21*, 395502.

(29) Perdew, J. P.; Burke, K.; Ernzerhof, M. Generalized Gradient Approximation Made Simple. *Phys. Rev. Lett.* **1996**, *77*, 3865–3868.

(30) Vanderbilt, D. Soft Self-Consistent Pseudopotentials in a Generalized Eigenvalue Formalism. *Phys. Rev. B* **1990**, *41*, 7892–7895.

(31) Grimme, S. Semiempirical GGA-Type Density Functional Constructed with a Long-Range Dispersion Correction. *J. Comput. Chem.* **2006**, *27*, 1787–1799.

(32) Barone, V.; Casarin, M.; Forrer, D.; Pavone, M.; Sambi, M.; Vittadini, A. Role and Effective Treatment of Dispersive Forces in Materials: Polyethylene and Graphite Crystals as Test Cases. *J. Comput. Chem.* **2009**, *30*, 934–939.

(33) Tersoff, J.; Hamann, D. R. Theory of the Scanning Tunneling Microscope. *Phys. Rev. B* **1985**, *31*, 805–813.

(34) Seufert, K.; Bocquet, M.-L.; Auwärter, W.; Weber-Bargioni, A.; Reichert, J.; Lorente, N.; Barth, J. V. Cis-Dicarbonyl Binding at Cobalt and Iron Porphyrins with Saddle-Shape Conformation. *Nat. Chem.* **2011**, *3*, 114–119.

(35) Kumagai, T.; Hanke, F.; Gawinkowski, S.; Sharp, J.; Kotsis, K.; Waluk, J.; Persson, M.; Grill, L. Thermally and Vibrationally Induced Tautomerization of Single Porphycene Molecules on a Cu(110) Surface. *Phys. Rev. Lett.* **2013**, *111*, 246101.

(36) Auwärter, W.; Écija, D.; Klappenberger, F.; Barth, J. V. Porphyrins at Interfaces. *Nat. Chem.* **2015**, *7*, 105–120.

(37) Kumagai, T. Direct Observation and Control of Hydrogen-Bond Dynamics Using Low-Temperature Scanning Tunneling Microscopy. *Prog. Surf. Sci.* **2015**, *90*, 239–291.

(38) Ladenthin, J. N.; Grill, L.; Gawinkowski, S.; Liu, S.; Waluk, J.; Kumagai, T. Hot Carrier-Induced Tautomerization within a Single Porphycene Molecule on Cu(111). *ACS Nano* **2015**, *9*, 7287–7295.

(39) Kumagai, T.; Ladenthin, J. N.; Litman, Y.; Rossi, M.; Grill, L.; Gawinkowski, S.; Waluk, J.; Persson, M. Quantum Tunneling in Real Space: Tautomerization of Single Porphycene Molecules on the (111) Surface of Cu, Ag, and Au. *J. Chem. Phys.* **2018**, *148*, 102330.

(40) Bischoff, F.; Seufert, K.; Auwärter, W.; Seitsonen, A. P.; Heim, D.; Barth, J. V. Metalation of Porphyrins by Lanthanide Atoms at Interfaces: Direct Observation and Stimulation of Cerium Coordination to 2H-TPP/Ag(111). *J. Phys. Chem. C* **2018**, *122*, 5083–5092.

TOC Graphics